

Topological zero-reflection points in multi-terminal quantum wire junctions

Abhiram Soori,^{1,*} Udit Khanna,² and Diptiman Sen³

¹*School of Physics, University of Hyderabad,
Prof. C. R. Rao Road, Gachibowli, Hyderabad 500046, India*

²*Theoretical Physics Division, Physical Research Laboratory, Navrangpura, Ahmedabad 380009, India*

³*Center for High Energy Physics, Indian Institute of Science, Bengaluru 560094, India*

We study scattering in noninteracting multi-terminal quantum wire junctions and show that junctions with dihedral symmetry can exhibit exact zero-reflection points for $N \geq 4$ terminals. By analyzing the scattering matrix, we identify these reflectionless points in the (E, t') parameter space, where E is the incident particle energy and t' is the junction hopping amplitude. These points exhibit an even-odd dependence on N and converge asymptotically to a common limiting value in the large- N limit. We show that the reflectionless points are characterized by an integer winding number associated with the phase of the reflection amplitude, providing a topological description for their stability against weak on-site disorder. We also consider junctions with broken time-reversal symmetry and find that a magnetic flux can induce additional reflectionless points, including for the $N = 3$ case. For a four-terminal junction threaded by a π -flux, we identify a unique parameter regime in which the reflection amplitude vanishes over the entire energy band. Finally, we discuss experimental signatures through the behavior of Friedel oscillations and examine the stability of these reflectionless points in the presence of weak interactions.

I. INTRODUCTION

The study of electron transport in quantum wire junctions has long been an important theme in condensed matter physics, spanning both noninteracting and interacting regimes [1–5]. In the noninteracting limit, symmetric junctions exhibit fundamental constraints on transport; for instance, a three-wire junction possesses a reflection probability bounded from below by $1/9$. This trend typically intensifies with the number of leads; for a symmetric junction where N wires meet at a single point, the reflection probability increases with N and asymptotically approaches unity in the large- N limit [1].

Such constraints prompt the fundamental question of whether it is possible to engineer a junction of N wires ($N \geq 4$) that supports zero-reflection transport. While a trivial solution exists for even N —attained by decoupling the junction into pairs of smoothly connected wires—it remains an open question whether a fully connected, non-trivial junction can host reflectionless states.

The search for reflectionless scattering modes is of significant interest across diverse physical platforms. In electromagnetism, such modes have been extensively investigated within the context of waveguides [6], while in condensed matter, they characterize the topological phase boundaries of the Andreev bound state spectrum in multi-terminal Josephson junctions [7]. In two-terminal setups, reflectionless points can lead to quantized charge pumping when

the system parameters are adiabatically driven along a closed contour encircling these points [8–10]. On the experimental front, the successful fabrication of multi-terminal quantum wire architectures [11] provides a viable platform for exploring such transport phenomena in the solid state.

In this work, we demonstrate that non-trivial reflectionless transport can be exactly realized in noninteracting multi-terminal quantum wire junctions. We identify specific coordinates in parameter space where the reflection amplitude vanishes identically, and we establish that these zeros are protected by a topological invariant. This underlying topological structure ensures the robustness of the reflectionless condition against weak perturbations, providing a rigorous framework for designing perfectly transmitting nodes in complex quantum networks. Furthermore, we reveal that a four-terminal junction threaded by a π -flux exhibits a broadband zero-reflection amplitude, yielding perfect transparency across the entire incident energy spectrum.

The remainder of this paper is organized as follows. In Sec. II, we present general symmetry considerations of the scattering matrix for N -terminal junctions, establishing the group-theoretic prerequisites for reflectionless transport. Section III details the microscopic tight-binding Hamiltonian and the exact scattering formalism used in our analysis. In Sec. IV, we provide explicit analytical and numerical results for the zero-reflection coordinates across various N -wire geometries, including their asymptotic behavior in the large- N limit. The underlying topological structure of these reflectionless points, characterized by an integer winding number, is established in Sec. V. We then examine the robust-

* abhirams@uohyd.ac.in

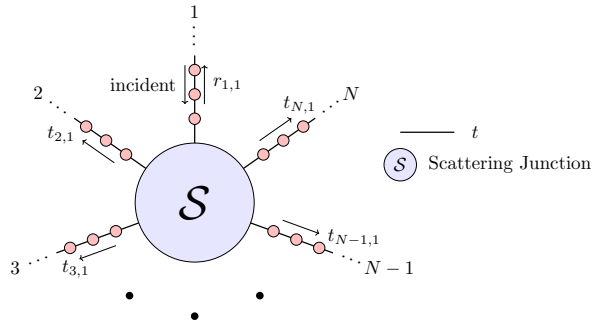


FIG. 1. Generic scattering junction \mathcal{S} coupled to N tight-binding wire leads.

ness of this topological protection against weak on-site disorder in Sec. VI, and explore the generation of reflectionless modes via time-reversal symmetry breaking in Sec. VII. Building on this, Sec. VIII investigates a four-terminal junction threaded by a π -flux, revealing the emergence of a broadband zero-reflection amplitude across the entire incident energy spectrum. In Sec. VIII, we briefly revisit the minimal $N = 2$ system to illustrate that these topological features manifest even in a simple two-terminal geometry with local impurities. Section IX discusses the physical implications of our findings, specifically proposing an experimental detection scheme via real-space Friedel oscillations and analyzing the stability of these zero-reflection fixed points under weak inter-particle interactions. Finally, we summarize our results and conclude in Sec. X.

II. GENERAL CONSIDERATIONS

Ballistic transport through a junction of N quantum wires is governed by the scattering matrix \mathcal{S} , that characterizes the junction as a function of the energy of the incoming electrons; in this work we will ignore the spin of the electrons for simplicity. The conservation of probability ensures that \mathcal{S} must be unitary at all energies (we ignore the possibility of inelastic scattering). Then we can examine the existence of reflectionless points in general N -terminal junctions very generally by studying $N \times N$ unitary matrices before considering a specific geometry of the junction in detail [12].

To set the stage for our analysis, we assume that N identical quantum wires, labeled as $n = 1, 2, \dots, N$, are connected to the junction with the same tunneling amplitude as shown in Figure 1. Then any of the wires (say, $n = 1$) can be chosen as the incident wire without loss of generality. In this case, the transmission amplitudes depends only on the symmetries of the junction. In this work, we shall focus

our attention to time reversal symmetric junctions. Then there are two geometric configurations possible: \mathcal{S} may be invariant under all elements of (i) the symmetric group on N wires S_N , or (ii) the dihedral group corresponding to the N -sided polygon D_N . Breaking time-reversal symmetry, say by introducing a flux through the junction, would reduce the symmetry to just the cyclic group of N elements C_N .

A. Full Symmetric Group

In this case, the junction is fully symmetric and immune to the geometric arrangement of the wires. Then all the transmission amplitudes are invariant under any pair-wise permutation (i, j) . Hence, \mathcal{S} comprises only two complex numbers r (the reflection amplitude) and t (the transmission amplitude). Then the most generic form of the scattering matrix for such a junction is,

$$\mathcal{S} = \begin{pmatrix} r & t & t & \dots & t \\ t & r & t & \dots & t \\ \vdots & \ddots & \vdots & \ddots & \vdots \\ t & t & t & \dots & r \end{pmatrix} \quad (1)$$

Without loss of generality, we can assume that r is real by adding an overall phase to \mathcal{S} which does not appear in any physical observables corresponding to a single junction. Imposing unitarity on \mathcal{S} , we find that \mathcal{S} is characterized by a single angle θ . We may write r, t as, $r = \cos \theta$, $t = e^{i\phi} \frac{1}{\sqrt{N-1}} \sin \theta$, which satisfies,

$$\tan \theta = -2 \frac{\sqrt{N-1}}{N-2} \cos \phi \quad (2)$$

A reflectionless point, $r = 0$, would correspond to $\theta = \pm \frac{\pi}{2}$ or $\tan \theta = \pm \infty$. However, $\cos \phi$ is bounded between -1 and 1 , and therefore $\tan \theta$ must be finite for all $N > 2$. Therefore, a fully symmetric multiterminal junction does not have any reflectionless points. In fact, the reflection coefficient, $r = \cos \theta = 1 - \frac{2}{N}$, approaches 1 for $N \gg 1$, implying that the junction becomes almost perfectly reflecting for large N . We note that this was demonstrated for the case of N wires connected to a single site in Ref. [1]. Here, we show that the result holds for any fully symmetric junction, irrespective of the microscopic structure.

B. Dihedral Group

Next, we consider junctions that have a somewhat lower symmetry – instead of being invariant under

any permutation of the incoming leads, we assume that the junction is invariant under the elements of the dihedral group D_N which describes the symmetries of an N -sided polygon. The generators of the group are rotation by $\frac{2\pi}{N}$ and a reflection. In the context of a multiterminal junction in which the leads are ordered as $1, 2, 3, \dots, N-1, N$, the former corresponds to a cyclic shift of the labels $(1, 2, \dots, N) \rightarrow (N, 1, 2, \dots, N-1)$, while the reflection about one of the leads (say about lead 1) corresponds to an interchange of the form $i \Leftrightarrow N+2-i$ (for $i > 1$), i.e., $(1, 2, \dots, N-1, N) \rightarrow (1, N, N-1, \dots, 3, 2)$. In this case, we have to analyze each N separately.

1. $N = 3$

Since the dihedral group D_3 is isomorphic to the symmetric group S_3 , we note that our results for the fully symmetric case immediately carry over (for a junction with three leads) if time-reversal symmetry is not broken. Therefore, such a junction does not have any reflectionless points. In fact, the minimal reflection amplitude is $r = 1 - \frac{2}{3} = \frac{1}{3}$. The case of time-reversal symmetry broken junctions is considered in section VII.

2. $N = 4$

$$\mathcal{S} = \begin{pmatrix} r & t_1 & t_2 & t_1 \\ t_1 & r & t_1 & t_2 \\ t_2 & t_1 & r & t_1 \\ t_1 & t_2 & t_1 & r \end{pmatrix} \quad (3)$$

As before, we assume (without loss of generality) that r is real, implying that there are 5 real parameters in \mathcal{S} . Imposing unitarity on \mathcal{S} , gives 3 equations of the form: $\mathcal{D} = 1, \mathcal{O}_1 = 0, \mathcal{O}_2 = 0$, where,

$$\mathcal{D} = r^2 + |t_2|^2 + 2|t_1|^2, \quad (4)$$

$$\mathcal{O}_1 = 2\text{Re}[rt_1 + t_1 t_2^*], \quad (5)$$

$$\mathcal{O}_2 = 2\text{Re}[rt_2] + |t_1|^2, \quad (6)$$

These equations can be satisfied by parameterizing the amplitudes as $r = \cos\theta$, $t_2 = e^{i\phi_2} \sin\theta \cos\psi$, and $t_1 = e^{i\phi_1} \sin\theta \sin\psi/\sqrt{2}$. Substituting these expressions into Eqs. (5) and (6) yields two relations among the four angular parameters. Imposing the zero-reflection condition, $r = 0$, requires $\sin\psi = 0$ and $\cos(\phi_1 - \phi_2) = 0$, which consequently yields $t_1 = 0$ and $t_2 = e^{i\phi_2}$. Physically, this indicates that wires 1 and 3 are perfectly coupled with vanishing reflection, while scattering from wire 1 into wires 2 and 4 is completely suppressed.

3. $N = 5$

Consider a 5-terminal junction with the dihedral symmetry D_5 . We label the wires $n = 1, 2, \dots, 5$ and assume that $n = 1$ is the incident wire. Due to the symmetry, there are 2 independent transmission amplitudes: $t_{2,1} = t_{5,1} = t_1$ and $t_{3,1} = t_{4,1} = t_2$. Then the S-matrix takes the form,

$$\mathcal{S} = \begin{pmatrix} r & t_1 & t_2 & t_2 & t_1 \\ t_1 & r & t_1 & t_2 & t_2 \\ t_2 & t_1 & r & t_1 & t_2 \\ t_2 & t_2 & t_1 & r & t_1 \\ t_1 & t_2 & t_2 & t_1 & r \end{pmatrix} \quad (7)$$

As before, we assume (without loss of generality) that r is real, implying that there are 5 real parameters in \mathcal{S} . Imposing unitarity on \mathcal{S} , gives 3 equations of the form: $\mathcal{D} = 1, \mathcal{O}_1 = 0, \mathcal{O}_2 = 0$, where,

$$\mathcal{D} = r^2 + 2|t_2|^2 + 2|t_1|^2, \quad (8)$$

$$\mathcal{O}_1 = 2\text{Re}(rt_1) + 2\text{Re}(t_1 t_2^*) + |t_2|^2, \quad (9)$$

$$\mathcal{O}_2 = 2\text{Re}(rt_2) + 2\text{Re}(t_1 t_2^*) + |t_1|^2, \quad (10)$$

Equation (8) can be satisfied if we parameterize the amplitudes as, $r = \cos\theta$, $t_2 = e^{i\phi_2} \frac{1}{\sqrt{2}} \sin\theta \cos\psi$, $t_1 = e^{i\phi_1} \frac{1}{\sqrt{2}} \sin\theta \sin\psi$. Plugging this in Eqs. (9) and (10), we find 2 relations between the 4 angles. Thus the scattering matrix can be parameterized by 2 real parameters.

A reflectionless point, $r = 0$, corresponds to $\theta = \pm\frac{\pi}{2}$ or $\tan\theta = \pm\infty$. Unlike the case of $N = 3$, here we find that it is possible to satisfy unitarity and $r = 0$ simultaneously. For the reflectionless point, we find,

$$r = 0, t_2 = \frac{e^{i\phi_2}}{2} \text{ and } t_1 = e^{i\frac{\pi}{3}} t_2. \quad (11)$$

To put this solution in perspective, we note that the solution above proves that a reflectionless point exists in the space of *all* allowed S-matrices with D_5 symmetry. Whether this is realized in a given microscopic realization for any set of parameters would depend on details of the specific junction.

4. $N = 6$

Consider a 6-terminal junction with the dihedral symmetry D_6 . As before we label the wires $n = 1, 2, \dots, 6$ and assume that $n = 1$ is the incident wire. Due to the symmetry, there are 3 independent transmission amplitudes: $t_{2,1} = t_{6,1} = t_1$, $t_{3,1} = t_{5,1} = t_2$ and $t_{4,1} = t_3$. Then the S-matrix takes the

form,

$$\mathcal{S} = \begin{pmatrix} r & t_1 & t_2 & t_3 & t_2 & t_1 \\ t_1 & r & t_1 & t_2 & t_3 & t_2 \\ t_2 & t_1 & r & t_1 & t_2 & t_3 \\ t_3 & t_2 & t_1 & r & t_1 & t_2 \\ t_2 & t_3 & t_2 & t_1 & r & t_1 \\ t_1 & t_2 & t_3 & t_2 & t_1 & r \end{pmatrix} \quad (12)$$

As before, we assume (without loss of generality) that r is real, implying that there are 7 real parameters in \mathcal{S} . Imposing unitarity on \mathcal{S} , gives 4 equations of the form: $\mathcal{D} = 1, \mathcal{O}_1 = 0, \mathcal{O}_2 = 0, \mathcal{O}_3 = 0$, where,

$$\mathcal{D} = r^2 + |t_3|^2 + 2|t_2|^2 + 2|t_1|^2, \quad (13)$$

$$\mathcal{O}_1 = 2\text{Re}(rt_1) + 2\text{Re}(t_2t_3^*) + 2\text{Re}(t_1t_2^*), \quad (14)$$

$$\mathcal{O}_2 = 2\text{Re}(rt_2) + 2\text{Re}(t_1t_3^*) + |t_1|^2 + |t_2|^2, \quad (15)$$

$$\mathcal{O}_3 = 2\text{Re}(rt_3) + 4\text{Re}(t_1t_2^*). \quad (16)$$

Equation (13) can be satisfied if we parameterize the amplitudes as, $r = \cos \theta$, $t_3 = e^{i\phi_3} \sin \theta \cos \psi$, $t_2 = e^{i\phi_2} \frac{1}{\sqrt{2}} \sin \theta \sin \psi \cos \beta$, $t_1 = e^{i\phi_1} \frac{1}{\sqrt{2}} \sin \theta \sin \psi \sin \beta$. Plugging this in Eqs. (14) and (16), we find 3 relations between the 6 angles. Thus the scattering matrix can be parameterized by 3 real parameters.

A reflectionless point, $r = 0$, corresponds to $\theta = \pm \frac{\pi}{2}$ or $\tan \theta = \pm \infty$. This may occur in two situations. First, a reflectionless point occurs for $\sin \psi = 0$, which means that all transmission amplitudes, except for t_3 , are vanish. This corresponds to a *trivial* reflectionless point, where the diagonally opposite wires are perfectly transmitting. Such a solution exists for all junctions with even N , including for $N = 4$ as we had seen before.

However, the $N = 6$ case presents an additional *non-trivial* reflectionless point, with partial transmission in all wires. This solution is parameterized by 2 angles:

$$r = 0, t_1 = \frac{e^{i\phi}}{\sqrt{2}} \sqrt{\frac{1 - \cos(2\beta)}{2 - \cos(2\beta)}} \sin(\beta), \quad (17)$$

$$t_2 = \pm \frac{ie^{i\phi}}{\sqrt{2}} \sqrt{\frac{1 - \cos(2\beta)}{2 - \cos(2\beta)}} \cos(\beta), \quad (18)$$

$$t_3 = \pm \frac{e^{i\phi}}{\sqrt{2 - \cos(2\beta)}}. \quad (19)$$

While these equations suggest, that there is a continuous family of reflectionless points, we emphasize that this only exists in the space of all S-matrices allowed by the symmetry. A given microscopic realization of a 6-terminal junction would only admit a subset of the complete space of S-matrices, and the trivial and/or non-trivial reflectionless points would exist only if the subset intersects this family.

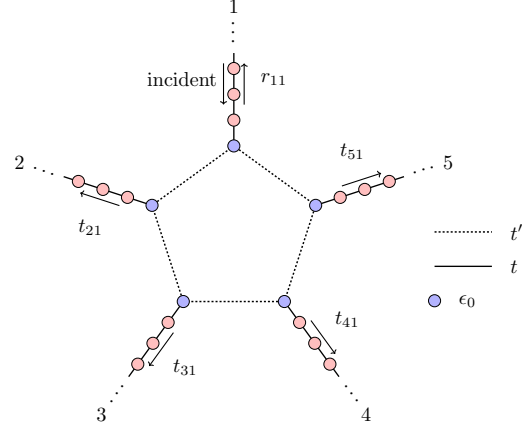


FIG. 2. Schematic picture of N -wire junction with $N = 5$ wherein each quantum wire is connected to two other wires. The first site of the chain has an on-site energy ϵ_0 , t' is the hopping amplitude that connects each quantum wire to two other wires and t is the hopping amplitude within each wire.

III. POLYGONAL JUNCTIONS

Following the general considerations in the previous section, we consider a specific microscopic model of junctions with dihedral symmetry. Specifically, we consider polygonal junctions (cf. Fig. 2) in which the junction is composed of N -sites arranged as a regular N -sided polygon. The system consists of N semi-infinite quantum wires connected to one another making a junction. The indices for lattice sites in each wire go from $m = 0$ to $m = \infty$. The Hamiltonian describing the system is given by

$$\begin{aligned} H = & -t \sum_{n=1}^N \sum_{l=0}^{\infty} (c_{n,l+1}^\dagger c_{n,l} + \text{H.c.}) \\ & -t' \sum_{n=1}^{n=N} (c_{n+1,0}^\dagger c_{n,0} + \text{H.c.}) \\ & + \epsilon_0 \sum_{n=1}^N c_{n,0}^\dagger c_{n,0}, \end{aligned} \quad (20)$$

where $c_{n,l}$ corresponds to annihilation of a particle at site l of n -th wire, t is the nearest neighbor hopping amplitude in each of the semi-infinite quantum wires, t' is the hopping amplitude that connects site-0 of n -th wire to site 0 of $(n+1)$ -th wire (note that $N+1 \equiv 1$) and ϵ_0 is the on-site energy for electrons on site 0 of each of the quantum wires. For simplicity, we set $t = 1$. (We will also set \hbar to unity in this paper). For wave functions of the form $e^{\pm ikl}$ in the wires, the dispersion is given by

$$E(k) = -2 \cos(ka), \quad (21)$$

where a is the lattice spacing (we will henceforth set $a = 1$). We study scattering of a plane wave incident on the junction with energy E from wire 1. The scattering eigenfunction for such a state has the form:

$$|\psi\rangle = \sum_{n=1}^N \sum_{l=0}^{\infty} \psi(n,l)|n,l\rangle, \quad \text{where}$$

$$\psi(n,l) = \begin{cases} e^{-ikl} + r_{1,1}e^{ikl} & \text{for } n = 1, \\ t_{n,1}e^{ikl} & \text{otherwise.} \end{cases} \quad (22)$$

Here, $k = \cos^{-1}(-E/2)$ lies in the range $0 < k < \pi$. (We do not include the values $k = 0$ and π since the group velocity $dE/dk = 0$ at those points). The time-independent Schrödinger equation $H|\psi\rangle = E|\psi\rangle$ for $\psi(n,0)$, with $n = 1, 2, \dots, N$ (where $N \geq 4$), give the equations

$$\begin{aligned} & - (e^{-ik} + r_{1,1}e^{ik}) - t' (t_{2,1} + t_{N,1}) \\ & + \epsilon_0 (1 + r_{1,1}) = E (1 + r_{1,1}), \\ & - t_{2,1}e^{ik} - t' (1 + r_{1,1}) - t' t_{3,1} \\ & + \epsilon_0 t_{2,1} = E t_{2,1}, \\ & - t_{N,1}e^{ik} - t' (1 + r_{1,1}) - t' t_{N-1,1} \\ & + \epsilon_0 t_{N,1} = E t_{N,1}, \\ & - t_{n,1}e^{ik} - t' t_{n-1,1} - t' t_{n+1,1} \\ & + \epsilon_0 t_{n,1} = E t_{n,1} \quad \text{for } 3 \leq n \leq N-1. \end{aligned} \quad (23)$$

Using these equations, the scattering coefficients $r_{1,1}$ and $t_{n,1}$ can be calculated.

We now study the condition for there to be no reflection, $r_{1,1} = 0$. Setting $t = 1$, we find that $r_{1,1} = 0$ will hold if the following conditions are satisfied:

$$\begin{aligned} & - t' (t_{2,1} + t_{N,1}) + e^{ik} + \epsilon_0 = 0, \\ & - t' - t' t_{3,1} + (e^{-ik} + \epsilon_0) t_{2,1} = 0, \\ & - t' - t' t_{N-1,1} + (e^{-ik} + \epsilon_0) t_{N,1} = 0, \\ & - t' t_{n-1,1} - t' t_{n+1,1} + (e^{-ik} + \epsilon_0) t_{n,1} \\ & = 0 \quad \text{for } 3 \leq n \leq N-1. \end{aligned} \quad (24)$$

The last equation in Eq. (24) has the general solution

$$\begin{aligned} t_{n,1} &= a_+(\lambda_+)^n + a_-(\lambda_-)^n, \\ \lambda_{\pm} &= \gamma \pm i \sqrt{1 - \gamma^2}, \\ \text{where } \gamma &= \frac{e^{-ik} + \epsilon_0}{2t'} \end{aligned} \quad (25)$$

and a_{\pm} are some constants. We note that λ_{\pm} satisfy the relation $\lambda_+ \lambda_- = 1$.

Since Eqs. (24) are symmetric under the $n \leftrightarrow N + 2 - n$, we can assume that the solutions of those equations have the same symmetry, namely,

$$t_{n,1} = t_{N+2-n,1} \quad \text{for } 1 \leq n \leq N+1, \quad (26)$$

where we define $t_{1,1} = t_{N+1,1} \equiv \psi(1,0) = 1$. We now separately discuss the cases where N is even and odd respectively.

(i) For $N = 2m$, we take

$$t_{n,1} = \frac{(\lambda_+)^{n-m-1} + (\lambda_+)^{m+1-n}}{(\lambda_+)^{-m} + (\lambda_+)^m}, \quad (27)$$

where $1 \leq n \leq N$, and we have used the relation $\lambda_- = 1/\lambda_+$. We find that Eq. (27) satisfies the symmetry in Eq. (26) and all the equations in Eq. (24) provided that

$$\frac{(\lambda_+)^{1-m} + (\lambda_+)^{m-1}}{(\lambda_+)^{-m} + (\lambda_+)^m} = \gamma^*. \quad (28)$$

(ii) For $N = 2m + 1$, we take

$$t_{n,1} = \frac{(\lambda_+)^{n-m-3/2} + (\lambda_+)^{m+3/2-n}}{(\lambda_+)^{-m-1/2} + (\lambda_+)^{m+1/2}}, \quad (29)$$

where $1 \leq n \leq N$, and we have used the relation $\lambda_- = 1/\lambda_+$. We find that Eq. (29) satisfies the symmetry in Eq. (26) and all the equations in Eq. (24) provided that

$$\frac{(\lambda_+)^{1/2-m} + (\lambda_+)^{m-1/2}}{(\lambda_+)^{-m-1/2} + (\lambda_+)^{m+1/2}} = \gamma^*. \quad (30)$$

Solving Eqs. (28) and (30), along with the expression for λ_+ given in Eq. (25) gives the reflectionless points as a function of N , t' , ϵ_0 and k .

In the following sections, we explicitly discuss a number of cases where there is no reflection.

IV. RESULTS

In this section, we present our results for various values of N , t' and k , for the case $\epsilon_0 = 0$. We will set $t = 1$.

A. $N = 4$

For $N = 4$, the scattering amplitudes take the forms,

$$\begin{aligned} r_{1,1} &= -\frac{e^{-i2k} (1 - 4t'^2 e^{-ik} \cos k)}{1 - 4e^{-2ik} t'^2}, \\ t_{2,1} = t_{4,1} &= \frac{2it' \sin k}{e^{2ik} - 4t'^2}, \\ t_{3,1} &= \frac{4it'^2 e^{-ik} \sin k}{e^{2ik} - 4t'^2}. \end{aligned} \quad (31)$$

It is clear that in the limit $t' \rightarrow \infty$ and with $k = \pi/2$, we have $r_{1,1} = t_{2,1} = t_{4,1} \rightarrow 0$ and $t_{3,1} \rightarrow -1$.

For general ϵ_0 , the conditions for zero-reflection are

$$E = 2\epsilon_0, \quad t' \rightarrow \pm\infty \quad (32)$$

At the zero-reflection points, $t_{3,1} = e^{2ik}$ and $t_{2,1} = t_{4,1} = 0$, where $k = \cos^{-1}(-E/2)$.

B. $N = 5$

For $N = 5$, we use Eq. (30) with $m = 2$. We find that the reflection amplitude $r_{1,1}$ is zero when either (i) $t' = 1$ and $k = \pi/3$, or (ii) $t' = -1$ and $k = 2\pi/3$.

For $N = 5$ and $\epsilon_0 \neq 0$, we find from Eq. (25) and Eq. (30) with $m = 2$ that there are reflectionless points when the following conditions are satisfied,

$$\begin{aligned} \frac{E}{2} &= \pm \sqrt{1 - \frac{3}{4} t'^2}, \\ \epsilon_0 &= \frac{t'}{2} \pm \sqrt{1 - \frac{3}{4} t'^2}, \end{aligned} \quad (33)$$

and in the second equation, we take the $+$ ($-$) sign in front of the square root if $t' < 0$ (> 0) respectively. For $\epsilon_0 = 0$, we recover the earlier results for reflectionless points at ($t' = 1, k = \pi/3$) and ($t' = -1, k = 2\pi/3$). Eq. (33) implies that the reflectionless points lie on ellipses in terms of either (t', ϵ_0) or (t', E) as shown in Fig. 3,

$$\begin{aligned} \frac{t' + E}{2} &= \epsilon_0 \\ \frac{3}{4} t'^2 + \frac{E^2}{4} &= 1. \end{aligned} \quad (34)$$

C. $N = 6$

For $N = 6$, we use Eq. (28) with $m = 3$. For $k = \pi/2$, we find that the reflection amplitude is zero if t' satisfies the equation

$$4(t')^4 - (t')^2 - 1 = 0. \quad (35)$$

The solution of this is given by

$$t' = \pm \sqrt{\frac{1 + \sqrt{17}}{8}} \simeq \pm 0.8002. \quad (36)$$

For $\epsilon_0 \neq 0$, the scattering eigenfunction corresponding to a particle incident from wire-1 has the following symmetry: $\psi(n, l) = \psi(6 - n + 2, l)$, which enforces $t_{n,1} = t_{6-n+2,1}$. The equations satisfied by the wavefunction $\psi(n, l)$ in Eq. (22) are

$$\begin{aligned} E\psi_{1,0} &= \epsilon_0\psi_{1,0} - \psi_{1,1} - t'(\psi_{2,0} + \psi_{6,0}) \\ E\psi_{2,0} &= \epsilon_0\psi_{2,0} - \psi_{2,1} - t'(\psi_{3,0} + \psi_{1,0}) \\ E\psi_{3,0} &= \epsilon_0\psi_{3,0} - \psi_{3,1} - t'(\psi_{4,0} + \psi_{2,0}) \\ E\psi_{4,0} &= \epsilon_0\psi_{4,0} - \psi_{4,1} - 2t'\psi_{3,0}, \end{aligned} \quad (37)$$

In these equations, substituting the form of the eigenfunction $\psi_{n,l}$ given in Eq. (22) and demanding $r_{1,1} = 0$ gives us the following equations for the locus of points in (t', ϵ_0, E)-space on which the reflection probability is zero:

$$2\epsilon_0 = E, \quad \epsilon_0^2 + t'^2 \left(\frac{8}{\sqrt{17} + 1} \right) = 1 \quad (38)$$

D. Larger values of N

The locations of the zero-reflection amplitude in the (k, t')-space, obtained numerically for $N \geq 7$, are summarized in Table I. An inspection of the data reveals a clear even-odd effect in the dependence on N .

For even values of N , the reflection probability R vanishes at $k = \pi/2$, provided t' is appropriately tuned to a value close to $\sqrt{3}/2$. In contrast, for odd values of N , the value of k at which $R = 0$ exhibits oscillations about $\pi/2$, with the amplitude of these oscillations decreasing as N increases for $t' = \sqrt{3}/2$.

A complementary behavior is observed for the hopping parameter t' . For odd $N > 10$, the condition $R = 0$ occurs at $t' \approx 0.8660$, whereas for even N , the corresponding values of t' oscillate around 0.8660, again with a diminishing amplitude as N increases.

| N | E | t' | R |
|-----|---------|--------|--------------------------|
| 7 | 0.3340 | 0.8860 | 1.3159×10^{-9} |
| 8 | 0.0000 | 0.8994 | 2.7493×10^{-9} |
| 9 | -0.113 | 0.8691 | 2.1046×10^{-9} |
| 10 | 0.0000 | 0.8570 | 1.2262×10^{-10} |
| 11 | 0.0382 | 0.8665 | 9.1902×10^{-10} |
| 12 | 0.0000 | 0.8693 | 1.5413×10^{-15} |
| 13 | -0.0133 | 0.8661 | 6.6776×10^{-9} |
| 14 | 0.0000 | 0.8650 | 1.6376×10^{-10} |
| 15 | 0.0045 | 0.8660 | 1.4159×10^{-9} |
| 16 | 0.0000 | 0.8664 | 1.663×10^{-10} |
| 17 | -0.0012 | 0.8660 | 7.3307×10^{-10} |
| 18 | 0.0000 | 0.8659 | 2.2536×10^{-10} |
| 19 | 0.0004 | 0.8660 | 3.1643×10^{-11} |
| 20 | 0.0000 | 0.8661 | 2.2649×10^{-11} |

TABLE I. Location of the zero-reflection amplitude in (E, t')-space evaluated numerically for various values of N , taking $\epsilon_0 = 0$ and $t = 1$. The last column shows the reflection probability R for the values of N , k and t' shown in the other columns. The number of digits on the right-side of decimal point shows the precision.

In the limit $N \rightarrow \infty$, both even and odd sequences converge to a common point, with vanishing reflection

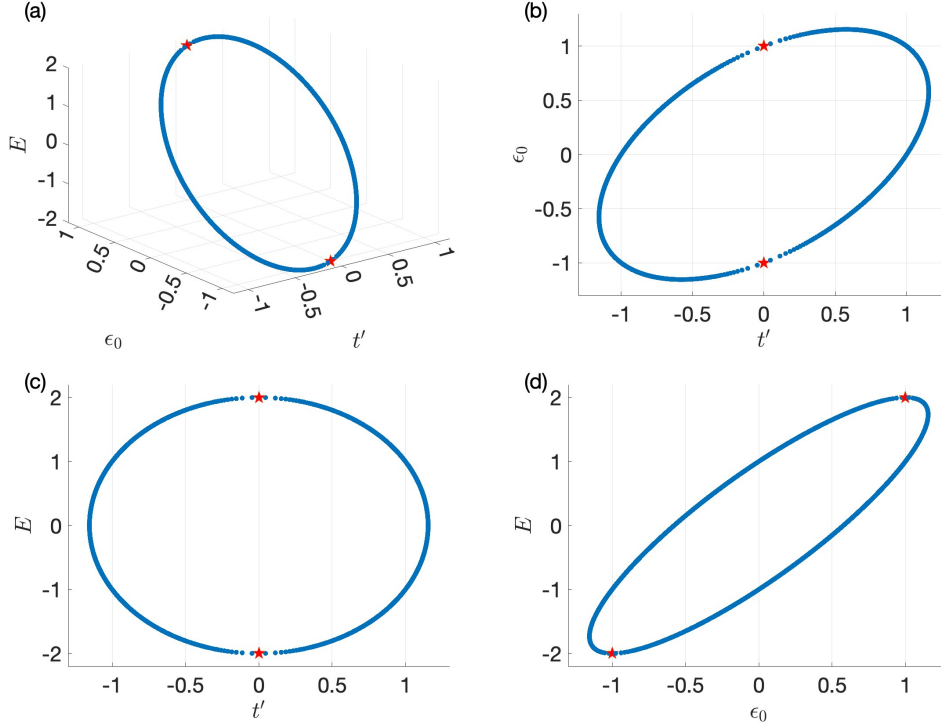


FIG. 3. Zero-reflection points for a junction with $N = 5$ wires. (a) Trajectories of the zero-reflection points in the (E, t', ϵ_0) parameter space. (b-d) Projections of the zero-reflection points onto the (b) (t', ϵ_0) , (c) (t', E) , and (d) (ϵ_0, E) planes.

tion occurring at $k = \pi/2$ and $t' = \sqrt{3}/2$. We now study how the reflectionless point shifts in the (t', k) plane when N is large.

For even values of N , it turns out that the reflectionless point remains at $k = \pi/2$, but t' shifts by a small amount which we can calculate as follows. First, we note that at $k = \pi/2$, Eq. (25) implies that

$$\lambda_{\pm} = -i\alpha \pm i\sqrt{1 + \alpha^2},$$

where $\alpha = \frac{1}{2t'}$. (39)

For $t' > 0$, we see that $|\lambda_+| < 1 < |\lambda_-|$. For large N , the dominant term in Eq. (28) leads to the condition

$$2t' \lambda_+ = i, \quad (40)$$

whose solution is given by $t' = \sqrt{3}/2$ and $\lambda_+ = i/\sqrt{3}$. Next, we compute the correction due to the subdominant terms. For $N = 2m$, Eq. (28) implies that

$$2t' \lambda_+ \left(\frac{1 + \lambda_+^{2m-2}}{1 + \lambda_+^{2m}} \right) = i. \quad (41)$$

For large m , we can set $\lambda_+ = i/\sqrt{3}$ in the terms λ_+^{2m-2} and λ_+^{2m} which are small, but we keep the

exact expression for $2t' \lambda_+ = i(\sqrt{1 + 4t'^2} - 1)$. This gives

$$\sqrt{4t'^2 + 1} - 1 = 1 - \frac{4}{3} \left(\frac{i}{\sqrt{3}} \right)^{N-2}. \quad (42)$$

We note that the factor of i^{N-2} in the correction term is real since N is even; however it oscillates in sign as N increases in steps of 2. We therefore see that for large N , the deviation of t' from $\sqrt{3}/2$ oscillates in sign and also goes to zero exponentially as $(1/\sqrt{3})^N$.

For odd values of $N = 2m + 1$, we find that the location of the reflectionless point shifts slightly from both $t' = \sqrt{3}/2$ and $k = \pi/2$. An analysis similar to the one given above for even N leads to the condition,

$$\begin{aligned} & \sqrt{4t'^2 - e^{-i2k}} - ie^{-ik} \\ &= -ie^{ik} \left[1 - \frac{4}{3} \left(\frac{i}{\sqrt{3}} \right)^{N-2} \right]. \end{aligned} \quad (43)$$

Note that the factor of i^{N-2} in the correction term is imaginary since N is odd; hence the value of k must necessarily differ from $\pi/2$. Eq. (43) implies that for large N , the deviations of t' and k from $\sqrt{3}/2$

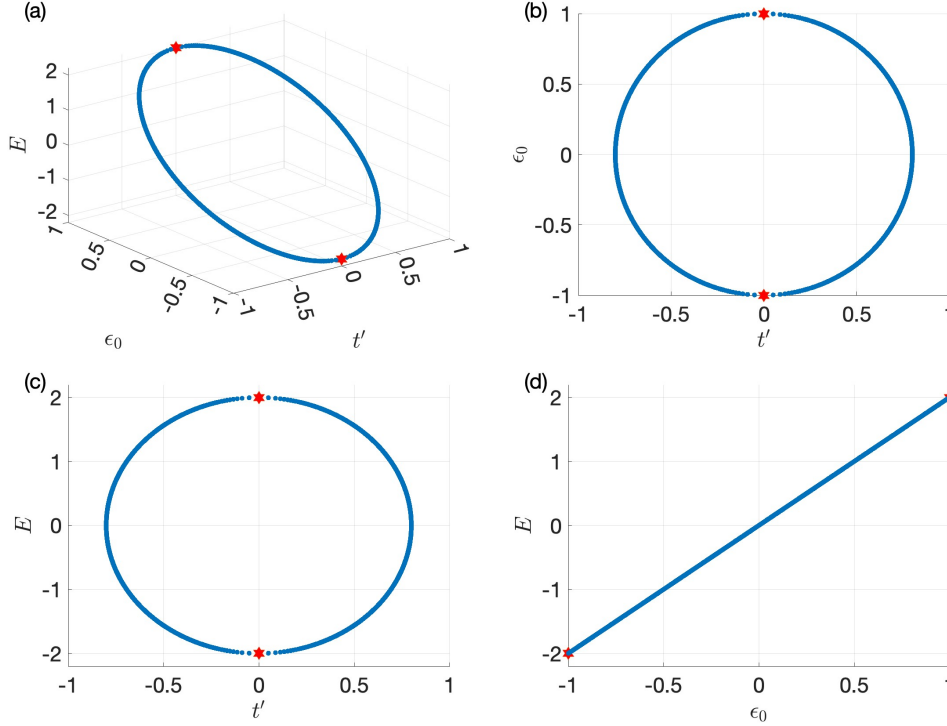


FIG. 4. Zero-reflection points for a junction with $N = 6$ wires. (a) Trajectories of the zero-reflection points in the (E, t', ϵ_0) parameter space. (b–d) Projections of these points onto the (b) (t', ϵ_0) , (c) (t', E) , and (d) (ϵ_0, E) planes. Red stars indicate the annihilation points where the zero-reflection condition is lifted and the reflection probability is !.

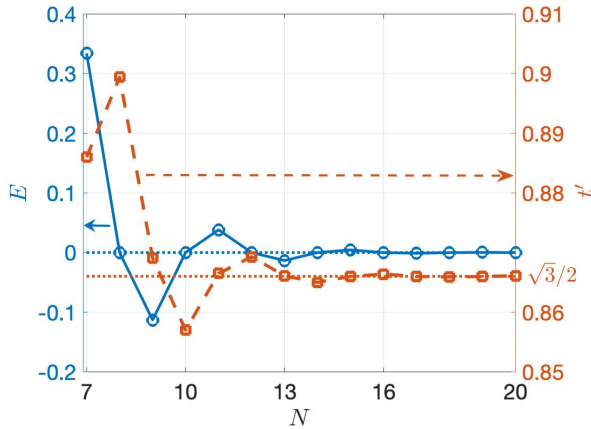


FIG. 5. Location of zero-reflection points as a function of N tabulated in Table I. It can be seen that in the limit of large N , zero-reflection point approaches $(E, t') = (0, \sqrt{3}/2)$.

and $\pi/2$ respectively both go to zero exponentially with N .

V. TOPOLOGICAL CHARACTERIZATION

The zero-reflection points in the (E, t') parameter space at a fixed ϵ_0 are associated with robust topological features. Specifically, the phase of the reflection amplitude evaluated along a closed loop encircling a zero-reflection point (E_0, t'_0) exhibits a winding of 2π . This behavior is a generic property of complex functions of two real variables and is fundamentally rooted in the argument principle of complex analysis [13].

In general, if the phase accumulated along a closed contour is $2\pi W_n$, the enclosed region contains $|W_n|$ zeros of the complex-valued reflection amplitude. Here, W_n is defined as the winding number for an incident electron from the wire labeled by n . Due to the symmetry of the junction, the scattering properties are independent of the choice of lead, rendering all W_n equal to one another. We therefore identify this integer as a universal topological invariant for the junction. To confirm the existence of these zeros, we compute the winding number for representative loops in (E, t') -space. A nonzero winding number provides a rigorous signature that the reflection amplitude vanishes at least once within the enclosed re-

gion. This topological characterization ensures that while numerical approximations may deviate slightly from the exact coordinates, the true zeros are topologically protected and must reside in the immediate vicinity of the numerically identified points.

We illustrate this for the case of $N = 5$ with $\epsilon_0 = 0$. In this regime, we identify two zero-reflection points in the (E, t') plane at $(-1, 1)$ and $(1, -1)$. These points possess winding numbers of $W_n = 1$ and $W_n = -1$, respectively, allowing them to be interpreted as a vortex and an antivortex. As $|\epsilon_0|$ increases toward unity, the vortex and antivortex approach one another in parameter space. Upon reaching $|\epsilon_0| = 1$, they undergo pair annihilation, after which the zero-reflection points vanish [see Fig. 3]. This annihilation occurs at the critical points $(t', \epsilon_0, E) = (0, \pm 1, \pm 2)$. Consequently, the trajectory of zero-reflection points in (E, t', ϵ_0) -space is continuous except at these specific annihilation coordinates.

VI. EFFECTS OF ON-SITE DISORDER

We now examine the stability of the zero-reflection points in the presence of on-site disorder at the central junction. On-site disorder is introduced by assigning random energies to the sites of the polygonal junction, drawn from a uniform distribution in the interval $[-w/2, w/2]$, where w denotes the disorder strength. Under weak disorder, the zero-reflection points in the (E, t') parameter space are slightly displaced but do not disappear. Crucially, the disorder breaks the N -fold rotational symmetry of the junction, which lifts the degeneracy of the reflection zeros across different leads. Consequently, the zero-reflection points associated with incidence from different wires no longer coincide but instead reside at distinct, lead-dependent locations. This behavior is illustrated in Fig. 6 for $N = 5$ with a disorder strength of $w = 0.1$ and a specific configuration: $(-0.0464, 0.0349, 0.0434, 0.0179, 0.0258)$.

The robustness of the zero-reflection condition against weak perturbations is a direct consequence of the underlying topological structure of the reflection amplitude. Since the winding number W_n is an integer-valued invariant, the zeros are topologically protected and cannot be eliminated by small perturbations that merely shift their coordinates in parameter space. However, in the strong-disorder regime, the behavior changes qualitatively. As w increases, the zero-reflection points for certain incident channels may eventually be destroyed—for instance, through pair annihilation—while they may persist for others, leading to channel-selective reflectionless transport.

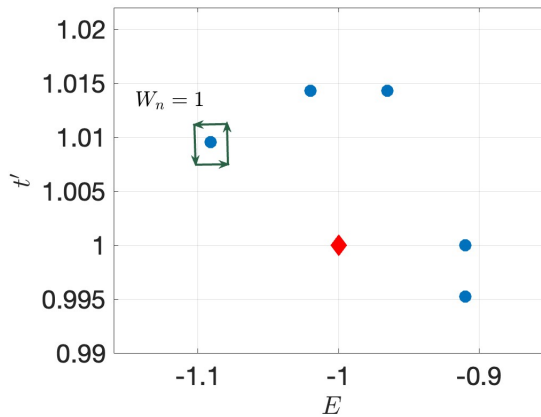


FIG. 6. Zero-reflection points for $N = 5$. The red diamond denotes the location of the zero-reflection point in the system without disorder ($w = \epsilon_0 = 0$). Blue circles indicate the shifted, lead-dependent locations of the zero-reflection points for a specific configuration of on-site disorder with strength $w = 0.1$. The disorder is drawn from a uniform distribution in the interval $[-w/2, w/2]$. Note that the disorder lifts the degeneracy of the zeros, causing them to occupy distinct positions in the (E, t') plane for different incident wires.

VII. EFFECTS OF TIME-REVERSAL SYMMETRY BREAKING

In this section, we consider what happens if time-reversal symmetry is broken at an N -wire junction, for example, by introducing a magnetic flux through the N -sided polygon. For $N = 3$ and 4 , we find that a flux can indeed give rise to reflectionless points which are not covered by the general discussion in Sec. II of junctions which are symmetric under time-reversal and reflection about one of the wires. We discuss these two cases below.

A. $N = 3$

We first consider a triangle with vertices labeled 1, 2 and 3 analogous to the $N = 5$ case depicted in Fig. 2. Setting $t = 1$ and $\epsilon_0 = 0$ in Eq. (20), we will study the condition for having zero reflection for an electron incident on one of the wires with an energy $E = -2 \cos k$, where $0 < k < \pi$. To describe the effect of a magnetic flux Φ through the triangle, we follow the Peierls prescription of introducing appropriate phases in the hopping amplitudes. Namely, the hopping amplitude between nearest neighbors in the anticlockwise direction (i.e., between pairs of sites $1 \rightarrow 2 \rightarrow 3 \rightarrow 1$) will have a phase $\phi/3$, where $\phi = q\Phi/(\hbar c)$ is the Aharonov-Bohm phase picked up

by the wave function of electrons going around the triangle (here q is the charge of an electron, and c is the speed of light). The nearest-neighbor hopping amplitude in the clockwise direction will then have a phase $-\phi/3$. Since ϕ is a periodic variable, we will assume that $-\pi \leq \phi \leq \pi$.

For an an electron incident on wire 1 and zero reflection, $r_{1,1} = 0$, Eqs. (24) take the form

$$\begin{aligned} t' (e^{-i\phi/3} t_{2,1} + e^{i\phi/3} t_{3,1}) - e^{ik} &= 0, \\ e^{i\phi/3} t' + e^{-i\phi/3} t' t_{3,1} - e^{-ik} t_{2,1} &= 0, \\ e^{-i\phi/3} t' + e^{i\phi/3} t' t_{2,1} - e^{-ik} t_{3,1} &= 0. \end{aligned} \quad (44)$$

These equations can be written in the matrix form

$$\begin{aligned} M_3 \begin{pmatrix} 1 \\ t_{2,1} \\ t_{3,1} \end{pmatrix} &= \begin{pmatrix} 0 \\ 0 \\ 0 \end{pmatrix}, \quad \text{where} \\ M_3 &= \begin{pmatrix} -e^{ik} & t'e^{-i\phi/3} & t'e^{i\phi/3} \\ t'e^{i\phi/3} & -e^{-ik} & t'e^{-i\phi/3} \\ t'e^{-i\phi/3} & t'e^{i\phi/3} & -e^{-ik} \end{pmatrix}. \end{aligned} \quad (45)$$

This will have a solution if $\det(M) = 0$. This gives the condition

$$2(t')^3 \cos(\phi) + 2(t')^2 \cos k + e^{-ik}((t')^2 - 1) = 0. \quad (46)$$

Since $\sin k \neq 0$, the imaginary part of the above expression being zero implies that we must have

$$t' = \pm 1. \quad (47)$$

The real part being zero then implies that

$$\cos k \pm \cos \phi = 0 \quad (48)$$

for $t' = \pm 1$ respectively.

We now assume that $t' = 1$. Given the ranges of k and ϕ specified above, we find that $t_{2,1} = 0$ and there is complete transmission from wire 1 to wire 3 with $t_{3,1} = -e^{i2\phi/3}$ if

$$-\pi < \phi < 0 \quad \text{and} \quad k = \pi + \phi. \quad (49)$$

By cyclic symmetry, there will also be complete transmission from wire 3 to wire 2 and from wire 2 to wire 1 when Eq. (49) is satisfied. The S -matrix for this system takes the form

$$\mathcal{S}_3 = -e^{i2\phi/3} \begin{pmatrix} 0 & 1 & 0 \\ 0 & 0 & 1 \\ 1 & 0 & 0 \end{pmatrix}. \quad (50)$$

Similarly, we find that if

$$0 < \phi < \pi \quad \text{and} \quad k = \pi - \phi, \quad (51)$$

then an electron incident on wire 1 will be completely transmitted to wire 2, from wire 2 to wire 3, and from wire 3 to wire 1, and the S -matrix is given by

$$\mathcal{S}'_3 = -e^{-i2\phi/3} \begin{pmatrix} 0 & 0 & 1 \\ 1 & 0 & 0 \\ 0 & 1 & 0 \end{pmatrix}. \quad (52)$$

The reflectionless points discussed above have a topological significance. If we hold ϕ fixed, we find that a small close curve in the (k, t') space which encircles the reflectionless point at $k = \pi \pm \phi$ and $t' = t$ has a non-zero winding number equal to 1.

B. $N = 4$

Next, we consider a square with vertices labeled 1, 2, 3 and 4 analogous to the $N = 5$ case depicted in Fig. 2. We put a phase of $-\phi/4$ and $\phi/4$ for nearest-neighbor hopping amplitude in the clockwise and anticlockwise directions respectively, so that the Aharonov-Bohm phase picked up in the anticlockwise direction is ϕ . We will look for the condition for having zero reflection for an electron incident on wire 1. Eq. (24) then gives the following matrix equation

$$\begin{aligned} M_4 \begin{pmatrix} 1 \\ t_{2,1} \\ t_{3,1} \\ t_{4,1} \end{pmatrix} &= \begin{pmatrix} 0 \\ 0 \\ 0 \\ 0 \end{pmatrix}, \quad \text{where} \\ M_4 &= \begin{pmatrix} -e^{ik} & t'e^{-i\phi/4} & 0 & t'e^{i\phi/4} \\ t'e^{i\phi/4} & -e^{-ik} & t'e^{-i\phi/4} & 0 \\ 0 & t'e^{i\phi/4} & -e^{-ik} & t'e^{-i\phi/4} \\ t'e^{-i\phi/4} & 0 & t'e^{i\phi/4} & -e^{-ik} \end{pmatrix}, \end{aligned} \quad (53)$$

where $k = \cos^{-1}[-E/2]$. This will have a solution if $\det(M) = 0$. It can be shown that this holds when

$$\begin{aligned} 2\epsilon_0 &= E, \\ 2t'^2 \left| \sin \frac{\phi}{2} \right| + \frac{E^2}{4} &= 1. \end{aligned} \quad (54)$$

Setting $t' = 1$ and $\epsilon_0 = 0$ for simplicity, we find that there are solutions at $k = \pi/2$ and $\phi = \pm\pi/3$. Choosing $\phi = \pi/3$, we find that $t_{2,1} = -e^{-i\pi/4}/\sqrt{3}$, $t_{3,1} = -1/\sqrt{3}$ and $t_{4,1} = e^{i\pi/4}/\sqrt{3}$, which implies that the transmission probabilities to wires 2, 3 and 4 are each equal to $1/3$. Using cyclic symmetry, we can then determine what happens if the electron is incident on wire 2, 3 or 4. We finally obtain the S -matrix for the system with $t' = 1$, $k = \pi/2$ and

$\phi = \pi/3$ as

$$\mathcal{S}_4 = \frac{1}{\sqrt{3}} \begin{pmatrix} 0 & e^{i\pi/4} & -1 & -e^{-i\pi/4} \\ -e^{-i\pi/4} & 0 & e^{i\pi/4} & -1 \\ -1 & -e^{-i\pi/4} & 0 & e^{i\pi/4} \\ e^{i\pi/4} & -1 & -e^{-i\pi/4} & 0 \end{pmatrix}. \quad (55)$$

Similarly, for $t' = 1$, $k = \pi/2$ and $\phi = -\pi/3$, we find that the S -matrix is given by

$$\mathcal{S}'_4 = \frac{1}{\sqrt{3}} \begin{pmatrix} 0 & -e^{-i\pi/4} & -1 & e^{i\pi/4} \\ e^{i\pi/4} & 0 & -e^{-i\pi/4} & -1 \\ -1 & e^{i\pi/4} & 0 & -e^{-i\pi/4} \\ -e^{-i\pi/4} & -1 & e^{i\pi/4} & 0 \end{pmatrix}, \quad (56)$$

which is the transpose of \mathcal{S}_4 in Eq. (55).

C. $N = 4$ and $\phi = \pi$

The π -flux junction for $N = 4$ yields striking scattering properties that can be derived analytically using the open-system retarded Green's function formalism [14]. Although $\phi = \pi$ corresponds to a time-reversal symmetric configuration (since $\phi = \pm\pi$ are identical), we note that this case lies beyond the scope of previous discussions of $N = 4$ junctions with dihedral symmetry in Secs. II B 2 and IV A. This is because for any polygonal junction with even N , a flux $\phi = \pi$ necessarily breaks the dihedral symmetry down to cyclic symmetry (assuming identical hopping amplitudes on all the bonds). For this reason, we study this case in the present section. The effective Hamiltonian of the four-site junction coupled to identical semi-infinite tight-binding leads is given by $H_{\text{eff}} = H_{4\pi} + \Sigma_L$, where the isolated central ring Hamiltonian with a symmetrically distributed π -flux is parameterized as

$$H_{4\pi} = -t' \begin{pmatrix} 0 & e^{-i\pi/4} & 0 & e^{i\pi/4} \\ e^{i\pi/4} & 0 & e^{-i\pi/4} & 0 \\ 0 & e^{i\pi/4} & 0 & e^{-i\pi/4} \\ e^{-i\pi/4} & 0 & e^{i\pi/4} & 0 \end{pmatrix}. \quad (57)$$

Because the four leads are structurally identical, the self-energy matrix is proportional to the identity operator, $\Sigma_L = \Sigma_0 I$, where $\Sigma_0 = -te^{ik}$ is the self-energy of an isolated one-dimensional tight-binding lead evaluated at the incident energy $E = -2t \cos k$.

The full retarded Green's function of the junction can be expressed in terms of an effective complex energy variable $z = E - \Sigma_0$ as

$$G^R(E) = (EI - H_{4\pi} - \Sigma_0 I)^{-1} = (zI - H_{4\pi})^{-1}. \quad (58)$$

Substituting the explicit forms of E and Σ_0 yields a compact expression for $z = -te^{-ik}$.

To evaluate the matrix elements analytically, we expand the resolvent using the algebraic identity $(zI - H_{4\pi})^{-1} = (zI + H_{4\pi})(z^2 I - H_{4\pi}^2)^{-1}$. The isolated Hamiltonian has a highly symmetric eigenspectrum with doubly degenerate eigenvalues at $\pm\sqrt{2}t'$. Consequently, its square is strictly proportional to the identity matrix, $H_{4\pi}^2 = 2t'^2 I$, an energy-independent constant. Noting that the diagonal elements of $H_{4\pi}$ vanish, the local Green's function at the injection site strictly evaluates to

$$G_{11}^R = \frac{z}{z^2 - 2t'^2} = \frac{-te^{-ik}}{t^2 e^{-2ik} - 2t'^2}. \quad (59)$$

The reflection amplitude r_k is governed by the standard scattering matrix relation $r_k = 1 - i\Gamma G_{11}^R$, where $\Gamma = -2\text{Im}(\Sigma_0) = 2t \sin k$ represents the hybridization escape rate into the continuum. Substituting G_{11}^R yields

$$r_k = 1 + \frac{2it^2 \sin k e^{-ik}}{t^2 e^{-2ik} - 2t'^2} = \frac{t^2 - 2t'^2}{t^2 e^{-2ik} - 2t'^2}. \quad (60)$$

Equation (60) is an important result. It shows a zero-reflection point with $r_k = 0$ can only exist when the numerator vanishes. This requires $2t'^2 = t^2$, or equivalently, $t' = t/\sqrt{2}$. Because the numerator is completely independent of the incident momentum k , this specific tuning of the junction hopping guarantees an extraordinary result that a zero-reflection amplitude, $r_k = 0$, occurs for all k . This implies that an arbitrary wave packet that is incident on any wire will not be reflected at all.

The cross-terminal transmission amplitudes follow directly from the off-diagonal elements of $G^R(E)$. Because the π -flux imposes a destructive interference node at the opposite terminal, $(H_{4\pi})_{31} = 0$, the corresponding Green's function element vanishes, $G_{31}^R = 0$. This guarantees $t_{3,1} = 0$ independent of the coupling t' or the momentum k .

Conversely, the transmission into the adjacent leads depends explicitly on the junction hopping amplitude t' and the specific flux distribution. Using $(H_{4\pi})_{21} = -t'e^{i\pi/4}$ and $(H_{4\pi})_{41} = -t'e^{-i\pi/4}$, we find

$$G_{21}^R = \frac{-t'e^{i\pi/4}}{t^2 e^{-2ik} - 2t'^2}, \quad G_{41}^R = \frac{-t'e^{-i\pi/4}}{t^2 e^{-2ik} - 2t'^2}. \quad (61)$$

The generic transmission amplitudes into leads 2 and 4 are thus given by

$$t_{2,1} = -i\Gamma G_{21}^R = \frac{2itt'e^{i\pi/4} \sin k}{t^2 e^{-2ik} - 2t'^2}, \quad (62)$$

$$t_{4,1} = -i\Gamma G_{41}^R = \frac{2itt'e^{-i\pi/4} \sin k}{t^2 e^{-2ik} - 2t'^2}.$$

In the limit $t' = t/\sqrt{2}$, the denominator simplifies exactly to $-2it^2 \sin k e^{-ik}$, allowing the transmission amplitudes to reduce to an optimal beam-splitting form dressed by the local phase structure of the junction,

$$t_{2,1} = -\frac{1}{\sqrt{2}}e^{i(k+\pi/4)}, \quad t_{4,1} = -\frac{1}{\sqrt{2}}e^{i(k-\pi/4)}. \quad (63)$$

VIII. ZERO-REFLECTION POINTS FOR $N = 2$

Consider a one-dimensional tight-binding chain with a uniform nearest-neighbor hopping amplitude $t = 1$. We introduce local impurities by defining the onsite energies at lattice sites $l = 0$ and $l = L$ as $\epsilon_0 - \delta$ and $\epsilon_0 + \delta$, respectively, where $\epsilon_0 \neq 0$. In this configuration, zero-reflection points emerge at isolated locations within the (E, δ) parameter space. Specifically, these points are strictly confined to the $\delta = 0$ axis, occurring at discrete energy values E that are determined by the impurity separation L .

The introduction of any finite asymmetry ($\delta \neq 0$) breaks the necessary condition, thereby destroying the zero-reflection points. However, despite their fragility to finite δ , these points possess an underlying topological character in the broader (E, δ) space. By calculating the phase of the reflection amplitude along a small closed loop enclosing a zero-reflection point, we find that the phase exhibits a quantized winding number of $W = \pm 1$, where the sign is strictly dictated by the sign of ϵ_0 . This non-trivial winding number characterizes the zero-reflection points as topological features, even in the simplest two-terminal geometry.

IX. FRIEDEL OSCILLATIONS IN DENSITY AND EFFECTS OF WEAK INTERACTIONS

In this section, we will discuss an observable signature of the reflectionless points that have been discussed above. We will show that Friedel oscillations [15–17] in the density in any wire vanishes when the Fermi momentum k_F coincides with a reflectionless momentum in that wire. We will then use this result to study what happens when the electrons interact weakly with each other in the wires [2, 18].

A. Friedel oscillations in density

We begin with a general discussion of Friedel oscillations. Consider an N -wire junction and let the

Fermi energy for the system be given by $E_F = -2t \cos k_F$, so that k_F is the Fermi momentum (this lies in the range $0 < k_F < \pi$ as usual). At zero momentum, the incoming states in all the wires will have all possible values of momentum lying in the range $0 \leq k \leq k_F$. The density at site l of the n -th wire is then given by the integral

$$\begin{aligned} \rho_{n,l} &= \int_0^{k_F} \frac{dk}{2\pi} \sum_{m=1}^N |\psi_{n,m,l}(k)|^2, \quad \text{where} \\ \psi_{n,m,l}(k) &\equiv t_{n,m}(k)e^{ikl} \quad \text{if } m \neq n, \\ \psi_{n,m,l}(k) &\equiv e^{-ikl} + r_{n,n}(k)e^{ikl} \quad \text{if } m = n. \end{aligned} \quad (64)$$

Physically, $\psi_{n,m,l}(k)$ denotes the contribution to the wave function at site l on wire n for a wave incident with unit amplitude with momentum k on wire m . We now concentrate on the first wire, labeled $n = 1$. The unitarity of the scattering matrix $\mathcal{S}(k)$ implies that

$$|r_{1,1}(k)|^2 + \sum_{m=2}^N |t_{1,m}(k)|^2 = 1 \quad (65)$$

for any value of k . Eq. (64) then leads to

$$\rho_{1,l} = \frac{k_F}{\pi} + \int_0^{k_F} \frac{dk}{2\pi} [r_{1,1}(k)e^{i2kl} + r_{1,1}^*(k)e^{-i2kl}]. \quad (66)$$

We now focus on the second term in Eq. (66),

$$\begin{aligned} \rho_{1,l,osc} &= \rho_{1,l} - \frac{k_F}{\pi} \\ &= \int_0^{k_F} \frac{dk}{2\pi} [r_{1,1}(k)e^{i2kl} + r_{1,1}^*(k)e^{-i2kl}]. \end{aligned} \quad (67)$$

We can use an approximation to analytically evaluate the expression in Eq. (67). We assume that $r_{1,1}(k)$ is independent of k and is given by its value at $k = k_F$, which we denote as $r(k_F)$ to simplify the notation. Then the integration in Eq. (66) approximately gives the oscillatory part of the density as

$$\rho'_{1,l,osc} = -\frac{i}{4\pi l} [r(k_F)e^{i2k_F l} - r^*(k_F)e^{-i2k_F l}], \quad (68)$$

where we have ignored the contribution from the lower limit, $k = 0$. We see from Eq. (68) that if $r(k_F) \neq 0$, $\rho'_{osc,1,l}$ oscillates with l with a wavelength equal to π/k_F , and its magnitude decays as $1/l$ for large l . If $r(k_F) = 0$, we have to return to Eq. (67) and redo the calculation. Typically, the derivative $dr_{1,1}(k)/dk \neq 0$ at $k = k_F$, and we then find that $\rho_{1,l,osc}$ again oscillates with a wavelength π/k_F , but its magnitude now decays as $1/l^2$ for large l .

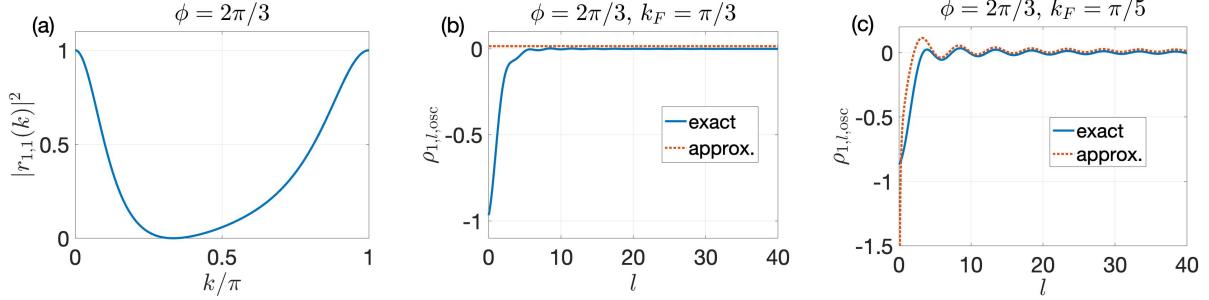


FIG. 7. Plots for a three-wire junction enclosing a flux $\phi = 2\pi/3$. There is no reflection when $k = \pi/3$. (a) Reflection probability in any wire versus k for the full range $0 < k < \pi$. (b) Oscillatory part of the density in any wire versus the site index l for $k_F = \pi/3$ which is a reflectionless point. The blue line denotes the exact numerical result, $\rho_{1,l,osc}$, obtained by integrating over k from 0 to k_F . The red line shows the approximate result, $\rho'_{1,l,osc}$, calculated using only the reflection amplitude at $k = k_F$. (c) Same plot as in (b) except that $k_F = \pi/5$ where $r(k_F) \neq 0$. The blue and red lines match very well for large values of l . The oscillations have a period equal to $\pi/k_F = 5$. In plots (b) and (c) the red curves are displaced upwards by 0.015 along the y -axis for contrast.

As an example, we consider a three-wire junction with a flux ϕ as discussed in Sec. VII A. We choose $\phi = 2\pi/3$, which gives a reflectionless point at $k = \pi/3$ according to Eq. (51). This is shown in Fig. 7 (a). Since the system has cyclic symmetry, the density $\rho_{n,l}$ will have the same form on all the wires. Fig. 7 (b) shows the numerically exact (Eq. (67)) and approximate (Eq. (68)) forms in blue and red respectively for $k_F = \pi/3$; the approximate form is exactly equal to zero since $r(k_F) = 0$. Fig. 7 (c) shows the numerically exact and approximate forms in blue and red respectively for $k_F = \pi/5$. We see that they match extremely well beyond about $l = 8$. As mentioned above, the oscillations have a period equal to $\pi/k_F = 5$.

In conclusion, the real-space particle density exhibits prominent Friedel oscillations whose amplitude decays as $1/l$ (where l is the distance from the junction) when the Fermi momentum deviates from the zero-reflection condition. Conversely, at the zero-reflection points, these spatial oscillations decay much more rapidly. Consequently, a systematic measurement of Friedel oscillations as a function of the Fermi momentum k_F provides a viable and non-invasive experimental signature for detecting and mapping these reflectionless points in multi-terminal quantum wire junctions.

B. Effects of weak interactions

We will now discuss the effects of weak interactions between the electrons in the wires following the method presented in Ref. [2]. The analysis is based on a continuum description of the wires; this is valid when the length scales of interest are all much larger than the lattice spacing $a = 1$. Further, we will work

in the vicinity of the Fermi momentum k_F , where the Fermi velocity of the electrons in the lattice model is given by $v_F = 2t \sin(k_F)$. We begin by introducing a dimensionless interaction parameter α_n in wire n . In the Tomonaga-Luttinger liquid description of spinless electrons with short-range density-density interactions in one dimension, the Luttinger parameters in wire n are related to α_n as

$$\begin{aligned} v_n &= v_F(1 - \alpha_n^2)^{1/2}, \\ K_n &= \left(\frac{1 - \alpha_n}{1 + \alpha_n} \right)^{1/2}, \end{aligned} \quad (69)$$

where v_n is the velocity of the bosonic (particle-hole) excitations, and K_n is the Luttinger parameter. For noninteracting electrons, we have $\alpha_n = 0$ and $K_n = 1$. For repulsive (attractive) interactions, $\alpha_n > 0$ (< 0) and therefore $K_n < 1$ (> 1) respectively.

We will simplify our notation by denoting the reflection amplitude in wire n as $r_{nn} = r_{n,n}(k_F)$ and the transmission amplitude from wire m to wire n as $t_{nm} = t_{n,m}(k_F)$. These define a scattering matrix S as usual. Next, we define a diagonal matrix F whose entries are given by

$$F_{nn} = -\frac{1}{2} \alpha_n r_{nn}. \quad (70)$$

Ref. [2] then shows that if $|\alpha_n| \ll 1$ (i.e., for weak interactions), the scattering matrix S (and therefore the matrix F whose elements are related to the diagonal elements of S) becomes a function of a distance scale L , and the variation of S with L is given by a renormalization group (RG) equation

$$\frac{dS}{dl} = SF^\dagger S - F, \quad (71)$$

where $l = \ln(L/a)$. Eq. (71) is only valid to first order in the α_n 's; these parameters do not themselves

flow under the RG. (One can check that Eq. (71) maintains the unitarity condition, $S^\dagger S = I$). We note that the derivation of Eq. (71) crucially uses the fact that Friedel oscillations in the density (in particular, the oscillations of the form $e^{\pm i2k_F x}$), lead to backscattering of electrons between incoming and outgoing states which lie at the momenta $-k_F$ and $+k_F$ [2, 18].

Eqs. (70) implies trivially that the matrix F vanishes if $r_{nn} = 0$ in all the wires. It then follows from Eq. (71) that S will not evolve under RG, at least to first order in α_n . Reflectionless points therefore have the remarkable property that they are fixed points of the RG flow when the interactions are weak.

Next, we study the stability of the fixed point at $r_{nn} = 0$. As a specific example, we consider the three-wire junction with a flux discussed in Sec. IX A. We choose a value of k_F which is slightly away from a reflectionless point, so that $|r_{nn}|$ is non-zero but small. We then numerically study how S evolves under Eq. (71). Taking all the α_n 's to be equal and positive (i.e., repulsive interactions), we find that $|r_{nn}|$ increases and eventually approaches 1 as the RG scale l grows. Hence, in this system, the reflectionless point is an unstable fixed point if the interactions are repulsive. In contrast, if we take the α_n 's to be equal and negative (i.e., attractive interactions), we find that $|r_{nn}|$ decreases and eventually approaches zero as l grows. Thus the reflectionless point is a stable fixed point for attractive interactions.

X. SUMMARY AND CONCLUSIONS

In this work, we have systematically investigated ballistic transport through N -terminal quantum wire junctions, revealing the existence of exact zero-reflection points. While fully symmetric junctions strictly forbid reflectionless scattering for $N \geq 3$, relaxing the symmetry constraints allows the reflection amplitude to vanish at specific, isolated coordinates within the (E, t') -space. Our numerical and analytical evaluations demonstrate a clear even-odd effect in the location of these points, which ultimately converge to $k = \pi/2$ and $t' = \sqrt{3}/2$ in the thermodynamic large- N limit.

Crucially, we established that these reflectionless coordinates possess a robust topological character, defined by an integer-valued winding number. This topological protection ensures that weak on-site dis-

order merely shifts the zero-reflection coordinates in parameter space—lifting the lead-dependent degeneracy due to the breaking of N -fold rotational symmetry—but does not immediately eliminate them. Annihilation of these points requires stronger perturbations that force the topological zero-reflection points (vortex and antivortex pair) to meet and mutually destroy one another.

Furthermore, we explored the effects of breaking time-reversal symmetry. By introducing a magnetic flux through the junction, we demonstrated that non-trivial reflectionless transport can be engineered even in geometrically constrained $N = 3$ and $N = 4$ systems. Most notably, in the specific case of an $N = 4$ junction threaded by a π -flux, we identified a broadband zero-reflection condition that yields perfect, energy-independent transmission, thereby significantly extending the versatility and reach of our proposed junction.

From an experimental and interacting perspective, these zero-reflection points leave distinct physical signatures. Specifically, the real-space Friedel oscillations in the particle density decay significantly faster when the Fermi momentum aligns with a zero-reflection point, providing a viable and non-invasive diagnostic tool for detecting these modes in solid-state devices. Additionally, we proved that these reflectionless coordinates serve as fixed points under renormalization group flow when subjected to weak inter-particle interactions.

Taken together, our results provide a comprehensive theoretical mechanism for realizing protected, reflectionless transport in noninteracting multi-terminal quantum junctions. These findings open new avenues for designing highly efficient quantum wire networks and manipulating topological scattering phases in scalable nanoelectronic architectures.

ACKNOWLEDGMENTS

AS acknowledges the financial support received from the Anusandhan National Research Foundation (erstwhile Science and Engineering Research Board) under the Core Research Grant (No. CRG/2022/004311), and from the University of Hyderabad. UK acknowledges support from the Physical Research Laboratory, Ahmedabad and the Department of Space, Government of India. We thank Arijit Saha for bringing Ref. [9] to our attention.

[1] E. Tan and R. Ganesh, Scattering off a junction, *Can. J. Phys.* **103**, 577 (2025).

[2] S. Lal, S. Rao, and D. Sen, Junction of several weakly interacting quantum wires: A renormaliza-

- tion group study, Phys. Rev. B **66**, 165327 (2002).
- [3] C. Chamon, M. Oshikawa, and I. Affleck, Junctions of three quantum wires and the dissipative Hofstadter model, Phys. Rev. Lett. **91**, 206403 (2003).
- [4] M. Oshikawa, C. Chamon, and I. Affleck, Junctions of three quantum wires, J. Stat. Mech.: Theory Exp. **2006** (02), P02008.
- [5] A. Soori and D. Sen, Conductance of Tomonaga-Luttinger liquid wires and junctions with resistances, EPL **93**, 57007 (2011).
- [6] W. R. Sweeney, C. W. Hsu, and A. D. Stone, Theory of reflectionless scattering modes, Phys. Rev. A **102**, 063511 (2020).
- [7] D. C. Ohnmacht, V. Wilhelm, and W. Belzig, Reflectionless modes as a source of Weyl nodes in multiterminal Josephson junctions (2025), arXiv:2503.10874 [cond-mat.mes-hall].
- [8] J. E. Avron, A. Elgart, G. M. Graf, and L. Sadun, Optimal quantum pumps, Phys. Rev. Lett. **87**, 236601 (2001).
- [9] O. Entin-Wohlman and A. Aharony, Quantized adiabatic charge pumping and resonant transmission, Phys. Rev. B **66**, 035329 (2002).
- [10] J. E. Avron, A. Elgart, G. M. Graf, and L. Sadun, Transport and dissipation in quantum pumps, J. Stat. Phys. **116**, 425 (2004).
- [11] A. R. Goni, L. N. Pfeiffer, K. W. West, A. Pinczuk, H. U. Baranger, and H. L. Stormer, Observation of quantum wire formation at intersecting quantum wells, Appl. Phys. Lett. **61**, 1956 (1992).
- [12] M. Hamermesh, *Group Theory and Its Application to Physical Problems*, Dover Books on Physics (Dover Publications, 2012).
- [13] J. W. Brown and R. V. Churchill, *Complex Variables and Applications*, 8th ed. (McGrawHill Higher Education, 2009).
- [14] S. Datta, *Quantum Transport: Atom to Transistor* (Cambridge University Press, Cambridge, UK, 2005).
- [15] J. Friedel, Metallic alloys, Il Nuovo Cimento (1955-1965) **7**, 287 (1958).
- [16] I. Tütto and A. Zawadowski, Quantum theory of local perturbation of the charge-density wave by an impurity: Friedel oscillations, Phys. Rev. B **32**, 2449 (1985).
- [17] R. Egger and H. Grabert, Friedel oscillations for interacting fermions in one dimension, Phys. Rev. Lett. **75**, 3505 (1995).
- [18] D. Yue, L. I. Glazman, and K. A. Matveev, Conduction of a weakly interacting one-dimensional electron gas through a single barrier, Phys. Rev. B **49**, 1966 (1994).